Published online 17 July 2007 *Nucleic Acids Research, 2007, Vol. 35, No. 15* ***4977–4988***
doi:10.1093/nar/gkm520

G-quadruplex induced stabilization by 2′-deoxy-2′-fluoro-D-arabinonucleic acids (2′F-ANA)

Chang Geng Peng and Masad J. Damha*

Department of Chemistry, McGill University, 801 Sherbrooke Street West, Montreal, QC, Canada H3A 2K6

Received April 28, 2007; Revised June 13, 2007; Accepted June 21, 2007

ABSTRACT

The impact of 2′-deoxy-2′-fluoroarabinonucleotide residues (2′F-araN) on different G-quadruplexes derived from a thrombin-binding DNA aptamer d($G_2T_2G_2TGTG_2T_2G_2$), an anti-HIV phosphorothioate aptamer PS-d($T_2G_4T_2$) and a DNA telomeric sequence d($G_4T_4G_4$) via UV thermal melting (T_m) and circular dichroism (CD) experiments has been investigated. Generally, replacement of deoxyguanosines that adopt the *anti* conformation (*anti*-guanines) with 2′F-araG can stabilize G-quartets and maintain the quadruplex conformation, while replacement of *syn*-guanines with 2′F-araG is not favored and results in a dramatic switch to an alternative quadruplex conformation. It was found that incorporation of 2′F-araG or T residues into a thrombin-binding DNA G-quadruplex stabilizes the complex (ΔT_m up to ~+3°C/2′F-araN modification); 2′F-araN units also increased the half-life in 10% fetal bovine serum (FBS) up to 48-fold. Two modified thrombin-binding aptamers (PG13 and PG14) show an approximately 4-fold increase in binding affinity to thrombin, as assessed via a nitrocellulose filter binding assay, both with increased thermal stability (~1°C/2′F-ANA modification increase in T_m) and nuclease resistance (4–7-fold) as well. Therefore, the 2′-deoxy-2′-fluoro-D-arabinonucleic acid (2′F-ANA) modification is well suited to tune (and improve) the physicochemical and biological properties of naturally occurring DNA G-quartets.

INTRODUCTION

Guanine quartet (G-quartet) structures with four Hoogsteen-paired, coplanar guanines were first observed more than 40 years ago (1) and later demonstrated to be a unique structural motif of guanine-rich oligonucleotides (2) (Figure 1A). G-quartets are found in nature and also in sequences identified by screening techniques such as *Systematic Evolution of Ligands by EXponential enrichment* (*SELEX*) (3–5). They have also aroused interest as therapeutic agents to inhibit human thrombin (6,7), HIV infection (7–9), and as targets themselves to inhibit telomerase activity in anticancer drug design (10).

G-quartets display extraordinary structural polymorphism (11–13). The 15-nt DNA sequence d($G_2T_2G_2TGTG_2T_2G_2$) (6) binds and inactivate thrombin, a key enzyme in the blood clotting cascade. NMR spectroscopy reveals that it adopts a uniquely folded structure with two stacked G-quartets connected through edge-loops (one TGT and two TT loops) involving antiparallel alignment of adjacent strands (Figure 1B) (14–17). A seemly different crystal structure of this aptamer–thrombin complex (18,19) was later analyzed to be in agreement with the previous NMR structure (19,20). Potassium ions stabilize the G-quadruplex by coordination to the G residues (15). The G-quartet displays an alternating *syn* and *anti* conformation of guanine bases (*syn*- and *anti*-Gs) on the same plane and 5′-*syn*-G/3′-*anti*-G along each strand of the quadruplex (i.e. 5′-*syn*-*anti*-3′ connectivity where *syn*-G includes G1, G5, G10 and G14 and *anti*-G includes G2, G6, G11 and G15 in Figure 1B) and all the thymidines are in the *anti* orientation (15).

The telomeric sequence d($G_4T_4G_4$) adopts symmetrical dimeric quadruplexes comprising four G-quartets linked through a diagonal loop as analyzed by NMR in sodium (Na^+) environment (Figure 1C) (21,22) or an edge-loop structure as revealed by X-crystallography in potassium (K^+) environment (23). More recent studies re-examined the crystal structure of this sequence and suggested the crystal structure also adopts a diagonal conformation, consistent with the NMR solution structure (24). The diagonal loop configuration (Figure 1C) consists of 5′-*syn*-G/3′-*anti*-G along each G-strand, *syn*-*syn*-*anti*-*anti* conformations in a G-quartet and all sugar residues puckered in the *south* (C2′-*endo*) conformation (22,25).

Another interesting example is the phosphorothioate oligonucleotide PS-d($T_2G_4T_2$) identified as an inhibitor of HIV-1 infection *in vitro* by combinatorial screening of a library of DNA strands. This aptamer inhibits HIV envelope-mediated cell fusion *in vitro* and its structure consists of a parallel-stranded tetramer with all guanines in the *anti*-conformation (Figure 1D) (2,7).

*To whom correspondence should be addressed. Tel: +1-514-398-7552; Fax: +1-514-398-3797; Email: masad.damha@mcgill.ca

Based on the above, the glycosidic conformations of guanines (i.e. *syn*- and *anti*-Gs) have a strong correlation with strand alignments. Parallel-stranded quadruplexes (Figure 1D) support only *anti*-G residues, while antiparallel-stranded quadruplexes favor alternating *syn-anti* Gs engaged in unimolecular (Figure 1B) or intermolecular complexes (Figure 1C) (11,26).

G-quadruplexes are sensitive to chemical modifications. Several studies aimed at modifying the thrombin-binding aptamer d($G_2T_2G_2TGTG_2T_2G_2$) have been reported (27–31), but very few, if any, have led to an improvement over the original molecule. For example, Seela and coworkers recently reported the insertion of a hairpin-forming sequence GCGAAG into the position of the central loop (TGT) of the thrombin-binding aptamer. This construct formed a G-quadruplex fused to a mini-hairpin structure. According to the T_m data, the mini-hairpin induces a structural change in the aptamer section, leading to less stable G-quadruplex. Binding to thrombin was not investigated (30). Saccà *et al*. studied the effect of backbone charge and atom size, base substitutions as well as the effect of modification at the sugar 2′-position as analyzed by spectroscopy. Fully modified aptamers with sugar modifications (ribose, 2′-*O*-methylribose) and phosphate backbone modifications (methylphosphonate, phosphorothioate) led to a reduction in the thermal stability (31). In fact, the 2′-*O*-methylribose modification led not only to a destabilization of the structure but to a complete transformation of the G-tetrad conformation, as shown by spectroscopy in potassium buffer (31). 2′-*O*-methylribose was also shown to causes structural changes in RNA aptamers and often resulted in a loss of activity (32). Accordingly, there is a need for new chemical modifications to improve the nuclease stability of this and other aptamers. Ideally, these modifications will not alter the subtle binding interactions of the selected native aptamers and the thermal stability of G-quadruplexes.

2′-Deoxy-2′-fluoro-D-arabinonucleic acids (2′F-ANA) confer DNA-like (*South*/*East*) conformations (33) to oligonucleotides while rendering them more nuclease resistant (34). The incorporation of 2′F-araN units in oligonucleotides also raises the T_m of different systems, i.e. duplexes ($\sim+1^\circ$C/nt) (35), triplexes ($\sim+0.8^\circ$C/nt) (36) and C-rich quadruplexes ($\sim+1^\circ$C/nt, pH <4.0) (37). In light of this and other advantageous characteristics of 2F-ANA, such as synthetic accessibility through

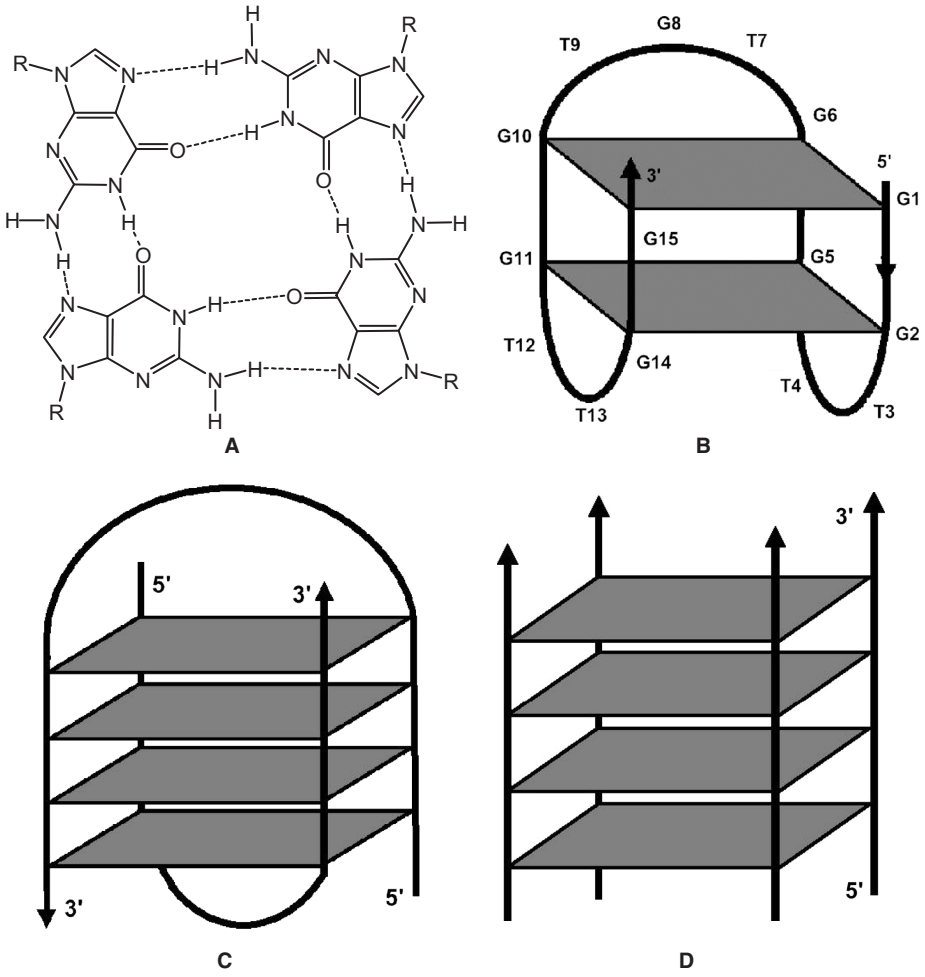

Figure 1. Structure of (**A**) G-quartet with cyclic array of four guanines linked by Hoogsteen H-bonds (1); (**B**) thrombin-binding DNA d($G_2T_2G_2TGTG_2T_2G_2$) with an edge-loop (chair-like) unimolecular G-quadruplex in K^+ (15,16); (**C**) a telomeric DNA d($G_4T_4G_4$) with diagonal-loop dimeric hairpin complex [d($G_4T_4G_4$)]$_2$ in Na^+ (21,22); (D) a tetrameric G-quadruplex [d(PS-$T_2G_4T_2$)]$_4$ with four parallel strands (2,7).

conventional solid-phase phosphoramidite chemistry, and promising antisense/siRNA properties (34,38–40), we have undertaken the first study concerning the ability of 2′F-ANA to form various G-quadruplex structures as analyzed by T_m and CD experiments. 2′F-ANA modified thrombin-binding aptamers were further evaluated by their nuclease resistance and binding affinity to thrombin. The outcome of these studies has opened new perspectives for the application of 2′F-ANA as aptamer oligonucleotides.

MATERIALS AND METHODS

Chemical synthesis of oligonucleotides

The sequence and composition of the oligomers prepared in this study are shown in Tables 1 and 2. Arabinose modified aptamer syntheses were carried out at a 1 μmol scale on an Applied Biosystems (ABI) 3400A synthesizer using standard β-cyanoethylphosphoramidite chemistry according to published protocols (41). Deoxyribonucleoside phosphoramidites were purchased from ChemGenes (Waltham, MA) and 2′F-arabinonucleoside 3′-*O*-phosphoramidites were provided by Topigen Pharmaceuticals Inc. (Montreal, Canada). The final concentrations of the monomers were 0.10 M for 2′-deoxyribonucleoside phosphoramidites and 0.125 M for the 2′F-arabinose phosphoramidites. The coupling time was extended to 150 s for the 2′-deoxyribonucleoside phosphoramidites dC and dG, and 15 min for the 2′F-araG and T phosphoramidites. These conditions gave about 99% average stepwise coupling yields. With the exception of PG17 through PG24, oligonucleotides were purified by anion-exchange HPLC (Waters Protein Pak DEAE-5PW column; 7.5 mm × 7.5 cm), desalted by size-exclusion chromatography on Sephadex G-25 resin, and characterized by MALDI-TOF mass spectrometry (Kratos Kompact-III Instrument; Kratos Analytical Inc., New York). Purity of the isolated oligonucleotides was >95% by HPLC. PG17–24 were used as obtained following deprotection and desalting.

UV thermal melting studies (T_m)

UV thermal dissociation data was obtained on a Varian CARY 1 spectrophotometer equipped with a Peltier temperature controller. Thrombin-binding aptamers (PG1–14) were dissolved in T_m buffer (10 mM Tris, pH 6.8, with and without 25 mM KCl) at a final concentration of 8 μM (42). Thrombin-binding aptamers were annealed in T_m buffer at 80°C for 10 min, allowed to cool to room temperature and refrigerated (4°C) overnight before measurements. $dT_2G_4T_2$ and related sequences (PG17–20) were dissolved in phosphate-buffered saline (PBS buffer, pH 7.2) composed of 137 mM NaCl, 2.7 mM KCl, 1.5 mM KH_2PO_4, 8 mM Na_2HPO_4 at a final concentration of 20 μM (43). The telomeric DNA $dG_4T_4G_4$ and related sequences (PG21–24) were dissolved in 10 mM sodium phosphate buffer (pH 7, 0.1 mM EDTA and 200 mM NaCl) at a final concentration of 100 μM (44). All samples (PG17–24) were annealed at 98°C for 5 min, naturally cooled down to room temperature and refrigerated (4°C) overnight before measurements. The annealed samples were transferred to pre-chilled Hellma QS-1.000 (Cat #114) quartz cell, sealed with a Teflon-wrapped stopper and degassed by placing them in

Table 1. Sequences, CD, T_m and binding data of 2′F-ANA modified thrombin-binding aptamers

Code	Type	Sequence[a]	T_m (ΔT_m)[b] (°C)	CD type[c]	Hysterisis in T_m[d]	K_d (nM)[e]	$t_{1/2}$ (h)[f]
PG1	All DNA	d(GGTTGGTGTGGTTGG)	46.4 [(42)] 47.4	II	no	210 200[(6)]	0.5
PG2	All 2′F-ANA	d(**GGTTGGTGTGGTTGG**)	54.1 (+0.4)	I	yes	500	>24
PG3	2′F-ANA G-*anti*	d(G**G**TTG**G**TGTG**G**TTG**G**)	53.3 (+1.5)	II	no	>700	4.8
PG4	2′F-ANA G-*anti*& loop	d(**GGTTGGTGTGGTTGG**)	61.6 (+1.3)	II	no	500	9.4
PG5	2′F-ANA G-*syn*	d(**GG**TTG**G**TGTG**G**TTG**G**)	45.4 (– 0.5)	I	yes	>700	0.8
PG6	2′F-ANA G-*syn*&loop	d(**GGTTGGTGTGGTTGG**)	48.5 (+0.1)	I	yes	>700	0.6
PG7	2′F-ANA G-quartet	d(**GGTTGGTGTGGTTGG**)	50.2 (+0.4)	I	yes	450	4.0
PG8	2′F-ANA all-loop	d(GG**TTGGTGTGGTT**GG)	56.3 (+1.3)	II	no	280	5.9
PG9	2′F-ANA loop	d(GG**TTGGTGTGGTT**GG)	57.1 (+1.6)	II	no	300	2.8
PG10	2′F-ANA loop	d(GG**TTGGTGTGGTT**GG)	51.2 (+0.8)	II	no	250	2.7
PG11	2′F-ANA loop	d(GG**TTGGTGTGGTT**GG)	56.6 (+1.8)	II	no	370	5.1
PG12	2′F-ANA loop	d(GG**TT**GGTGTGG**TT**GG)	59.1 (+2.9)	II	no	310	3.5
PG13	2′F-ANA loop	d(GGTTGG**TGTGGTT**GG)	51.0 (+0.9)	II	no	58	3.4
PG14	2′F-ANA loop	d(GG**TTGGTGTGGTT**GG)	50.6 (+0.8)	II	no	40	2.0
P8	ssDNA control	d(GTCTCTTGTGTGACTCTGGTAAC)	NA	NA	NA	NC	0.5
H1	Hairpin control (RNA)	r(GGACUUCGGUCC)	NA	NA	NA	NC	NA

[a]Capital and bold letter: **2′F-ANA**.
[b]ΔT_m is the T_m change per each 2′F-ANA residue between any modified aptamer with the unmodified DNA aptamer (PG1, T_m = 47.4°C); NA: not applicable.
[c]'Type I' CD spectrum refers to a positive CD band at ~265 nm and a negative band at ~240 nm that correlates with G-anti conformation in the G-quartet. 'Type II' CD refers to a CD spectrum with positive band at ~295 nm and a negative band at ~260 nm, which indicates a mixed *anti*-G and *syn*-G conformation in the G-quartet. CD was measured in the buffer of 10 mM Tris, pH 6.8, 25 mM KCl (12).
[d]Hysterisis in T_m refers to the hysterisis existing between a heating and cooling process with 0.5°C/min temperature change during T_m measurements.
[e]K_d was roughly estimated from the concentration (nM) where 50% of the maximum binding percentage was observed with a certain aptamer during the thrombin concentrations studied; NC: not calculated.
[f]Half-life in 10% fetal bovine serum (FBS) as monitored by 20% polyacrylamide gel electrophoresis.

Table 2. CD and T_m data of d($T_2G_4T_2$) and d($G_4T_4G_4$) and related oligonucleotides

Code	Type	Sequence[a]	CD Type[b,c]	T_m[d] (ΔT_m)[e] (°C)
d($T_2G_4T_2$) and related sequences				
PG17	All PO-DNA	PO-d(TTGGGGTT)	I	66.0
PG18	All PS-DNA	PS-d(TTGGGGTT)	I	73.5[43] 74.0
PG19	All PS-2′F-ANA	PS-d(**TTGGGGTT**)	I	83.0 (+1.1)
PG20	PS-2′F-ANA-G	PS-d(TT**GGGG**TT)	I	87.0 (+3.3)
d($G_4T_4G_4$) and related sequences				
PG21	All PO-DNA	PO-d(GGGGTTTTGGGG)	II	65[44] 64.4
PG22	All PO-2′F-ANA	PO-d(**GGGGTTTTGGGG**)	I	90.0 (+2.1)
PG23	G-*syn*	PO-d(**GGG**GTTTT**GGG**G)	I	72.5 (+2.0)
PG24	G-*anti*	PO-d(G**GGG**TTTTG**GGG**)	II	66.2 (+0.5)

[a]Capital and bold letter: **2′F-ANA**; PO: phosphate linkage; PS: phosphorothioate linkage.
[b]CD type I & II refer to the note in Table 1.
[c]d$T_2G_4T_2$ and related sequences (PG17–20): phosphate-buffered saline (PBS buffer, pH 7.2 at 25°C), 137 mM NaCl, 2.7 mM KCl, 1.5 mM KH_2PO_4, 8 mM Na_2HPO_4; strand concentration: 20 μM for both CD and T_m experiments. d$G_4T_4G_4$ and related sequences (PG21–24): 10 mM sodium phosphate buffer, 0.1 mM EDTA, pH 7 and 200 mM NaCl; strand concentration: 10 μM.
[d]d$T_2G_4T_2$ and related sequences (PG17–20): phosphate-buffered saline (PBS buffer, pH 7.2 at 25°C), 137 mM NaCl, 2.7 mM KCl, 1.5 mM KH_2PO_4, 8 mM Na_2HPO_4; strand concentration: 20 μM; T_m data were generated from concentration-dependent CD spectra (Figure S5 and 'Materials and methods' section). d$G_4T_4G_4$ and related sequences (PG21–24): 10 mM sodium phosphate buffer, 0.1 mM EDTA, pH 7 and 200 mM NaCl; strand concentration: 100 μM; T_m measurements were conducted at 295 nm wavelength.
[e]ΔT_m (°C) is the T_m change/2′F-ANA modification of PG18–20 or PG22–24 relative to the control PG18 (74.0°C) or PG21 (PG64.4°C), respectively.

an ultrasonic bath for 1 min. Extinction coefficients were obtained from the following internet site (http://www.idtdna.com/analyzer/applications/oligoanalyzer) based on the nearest-neighbor approach (45) and modified aptamers (phosphorothioates and 2′F-ANA) were assumed to have the same extinction coefficient as the natural DNA aptamer. Denaturation/cooling curves were acquired at either at 295 nm for d($G_2T_2G_2TGTG_2T_2G_2$) and related sequences (PG1–14), d$G_4T_4G_4$ and related sequences (PG21–24), or at 260 nm for d$T_2G_4T_2$ and related sequences (PG17–20), at a heating/cooling rate of 0.5°C/min between 10 and 80°C (for PG1–14), 20 and 90°C (for PG17–20) or 40 and 98°C (for PG21–24). The data were analyzed with the software provided by Varian and converted to Microsoft Excel (Tables 1 and 2). The decreases in UV absorbance (hypochromicity) with increasing temperature were normalized between 1 and 0 by the formula: $N = (A_t - A_l)/(A_h - A_l)$, where A_t is the absorbance at any given temperature (t), A_l is the minimum absorbance reading at high temperature and A_h is the maximum absorbance reading at low temperature. T_m concentration dependence studies were also conducted in the same way at 295 nm using thrombin-binding aptamers (PG1–14) with different concentrations ranging from 4 to 76 μM. Starna quartz cells (Starna Cells, Inc., Cat. # 1-Q-1) with 1-mm path length were used at high concentrations to reduce the amount of aptamers required and to avoid exceeding the Absorbance range of the instrument.

Circular dichroism (CD) spectra

CD spectra (200–320 nm) were collected on a Jasco J-710 spectropolarimeter at a rate of 100 nm/min using fused quartz cells (Hellma, 165-QS). Measurements were carried out either in 10 mM Tris, pH 6.8 (with and without 25 mM KCl) at a concentration of 8 μM for thrombin-binding aptamers (PG1–14) (42); in PBS buffer (pH 7.2, 137 mM NaCl, 2.7 mM KCl, 1.5 mM KH_2PO_4, 8 mM Na_2HPO_4) for d$T_2G_4T_2$ and related sequences (PG17–20) at a final concentration of 20 μM (43), or in sodium phosphate buffer (10 mM sodium phosphate buffer, pH 7, 0.1 mM EDTA and 200 mM NaCl) for d$G_4T_4G_4$ and related sequences (PG21–24) at a final concentration of 100 μM (44). Temperature was controlled by an internal circulating bath (VWR Scientific) at constant temperature. The data was processed using J-700 Windows software supplied by the manufacturer (JASCO, Inc.). To facilitate comparisons, the CD spectra were background subtracted, smoothed and corrected for concentration so that molar ellipticities could be obtained. Temperature-dependent CD spectra were also conducted for d$T_2G_4T_2$ and related sequences (PG17–20). A 10-min equilibration time was allowed at each temperature before CD scanning. The T_m profile was obtained by plotting the maximum molar ellipticities versus temperature and normalizing.

Nuclease stability assay

Nuclease stability of anti-thrombin aptamers was conducted in 10% fetal bovine serum (FBS, Wisent Inc., Cat. #080150) diluted with multicell Dulbecco's Modified Eagle's Medium (DMEM, Wisent Inc., Cat. #319005-CL) at 37°C. A single-strand DNA (ssDNA) 23mer (P-8), which is unable to form G-quadruplexes, was used as a control. Approximately 8 μmol of stock solution of aptamers and ssDNA control (~1.2 O.D.U) was evaporated to dryness under reduced pressure and then incubated with 300 μl 10% FBS at 37°C. At 0, 0.25, 0.5, 1, 2, 6 and 24 h, 50 μl of samples were collected and stored at –20°C for at least 20 min. The samples were evaporated to dryness and then 10 μl of gel loading buffer and 10 μl of

autoclaved water was added. 10 µl of the mixture was used for polyacrylamide gel electrophoresis (PAGE), which was carried out at room temperature using 20% polyacrylamide gel in 0.5× TBE buffer (Tris-borate-EDTA). The degradation patterns on the gels were visualized using Stains-All (Bio-Rad) according to the manufacturer's protocol.

5′-End labeling of synthetic oligonucleotides

Aptamers (PG1–14) were radiolabeled at the 5′-hydroxyl terminus with a radioactive ^{32}P probe using a T4 polynucleotide kinase (T4 PNK) according to the manufacture's specifications (MBI Fermentas Life Sciences, Burlington, ON). Incorporation of the ^{32}P label was accomplished in reaction mixtures consisting of DNA aptamers substrate (100 pmol), 2 µl 10 × reaction buffer (500 mM Tris–HCl, pH 7.6 at 25°C, 100 mM $MgCl_2$, 50 mM DTT, 1 mM spermidine and 1 mM EDTA), 1 µl T4 PNK enzyme solution (10 U/1µl in a solution of 20 mM Tris–HCl, pH 7.5, 25 mM KCl, 0.1 mM EDTA, 2 mM DTT and 50% glycerol), 6 µl [γ-^{32}P]-ATP solution (6000 Ci/mmol, 10 mCi/ml; Amersham Biosciences, Inc.) and autoclaved sterile water to a final volume of 20 µl. The reaction mixture was incubated for 30–45 min at 37°C, followed by a second incubation for 5 min at 95°C to thermally denature and deactivate the kinase enzyme. The solution was purified according to a standard protocol (46) and the isolated yield of ^{32}P-5′-DNA following gel extraction averaged 50%. The pure labeled samples were kept at –20°C for future use.

Nitrocellulose filter binding assay

Labeled aptamers (1.25 pmol) were heated to 95°C for 5 min in the binding buffer (Tris–Ac, pH 7.4, 140 mM NaCl, 5 mM KCl, 1 mM $CaCl_2$, 1 mM $MgCl_2$) (6) and immediately placed on ice for 5 min before binding to increasing concentrations of thrombin protease (Amersham Biosciences, Inc.) ranging from 10 to 1000 nM in the binding buffer at 37°C in a final volume of 20 µl for 30 min. Mixtures were filtered through a nitrocellulose filter (13 mm Millipore, HAWP, 0.45 µm) pre-wetted with binding buffer in a Millipore filter binding apparatus, and immediately rinsed with 600 µl ice-cold washing buffer [Tris–Ac, pH 7.4, 140 mM NaCl, 5 mM KCl, 1 mM $CaCl_2$, 1 mM $MgCl_2$, 1% sodium pyrophosphate (w/v)], then the filter was air-dried and the bound aptamer quantified by scintillation counting. The binding percentage (%) was calculated by the subtraction of the background from the counts in the microtube. K_d was roughly estimated from the concentration (nM) where 50% of the maximum binding percentage was observed with a certain aptamer during the thrombin concentrations studied.

RESULTS AND DISCUSSION

Oligonucleotide aptamers derived from SELEX have drawn great attention for their potential as therapeutic and diagnostic agents (47–50). The application of nucleic acid aptamers *in vivo* and their possible use in pharmacotherapy face the same key hurdles as siRNA and antisense based therapeutics, e.g. delivery, cellular uptake and biostability. To date, several methods have been devised to improve the stability of aptamers, most of which make use of SELEX, including a mirror-design of RNA aptamers (or 'Spiegelmers') (51); post-SELEX modification by 2′-OMe to increase the stabilization of RNA aptamers (32); and direct evolution in SELEX using modified dNTPs or rNTPs (e.g. 2′-F, 2′-NH_2 pyrimidine 5′-triphosphate) (52–56). Macugen®, an aptamer recently approved by the FDA for the treatment of neovascular age-related macular degeneration, is a 2′F/2′-OMe ribose-modified oligomer (57). There still exists a great demand for new methods and more diverse range of chemistries to create aptamers with more favorable pharmacokinetic properties.

A fully 2′F-ANA modified thrombin-binding aptamer

The study began with the replacement of all the deoxynucleotides in the thrombin-binding aptamer d($G_2T_2G_2TGTG_2T_2G_2$) by 2′F-ANA units. Consistent with literature results (15,42), it was found through comparisons of the T_m profiles both with and without the presence of K^+, that potassium ions stabilized the unimolecular G-quadruplex of the DNA aptamer (PG1) (Figure 2A and B). As shown in the literature, similar hypochromicity (UV absorbance decrease with increased temperature) was observed at 295 nm for all DNA sequence (42), which is an indication of G-quartet formation (12,58). The T_m of the all DNA aptamer obtained in this study was 47.4°C (Table 1 and Figure 2B), consistent with 46.4°C reported by Smirnov and Shafe (42) and the CD spectra also support the UV melting experiment. Previous studies have shown two typical CD spectra: a CD spectrum with a positive CD band at ~265 nm and a negative band at ~240 nm (Type I CD spectrum) is related to a parallel quadruplex with all *anti*-Gs, while one with a positive band at ~295 nm and a negative band at ~260 nm (Type II CD spectrum) corresponds to antiparallel quadruplex with alternating *syn-anti* Gs (12). The all DNA aptamer shows very low amplitude bands without K^+, whereas it demonstrates characteristic Type II CD when K^+ is present, indicating a G-quadruplex structure with alternating *syn-anti* Gs (Figure 2C and D) (11,12). The lack of concentration dependence in the T_m data (Figure 3) and the lack of hysteresis in the heating/cooling processes (Figure 4) support a unimolecular G-quadruplex structure (Figure 1B). Lack of hysteresis at a heating/cooling rate of 0.5°C/min indicates a fast kinetics for the formation of unimolecular quadruplexes (58).

The all 2′F-ANA aptamer (PG2) also forms a defined G-quadruplex stabilized by K^+ in the UV melting experiment (Figure 2A and B). The G-quadruplex of all 2′F-ANA aptamer (PG2) is more thermally stable than the all DNA aptamer (PG1) (ΔT_m = 0.4°C/2′F-ANA modification in Table 1). Further characterization experiments indicated that the G-quadruplex PG2 formed in K^+ is different from that of that of PG1. The effect of K^+ on the CD spectra is consistent with the T_m experiment: very low absorbance in the absence of K^+ and a strong positive

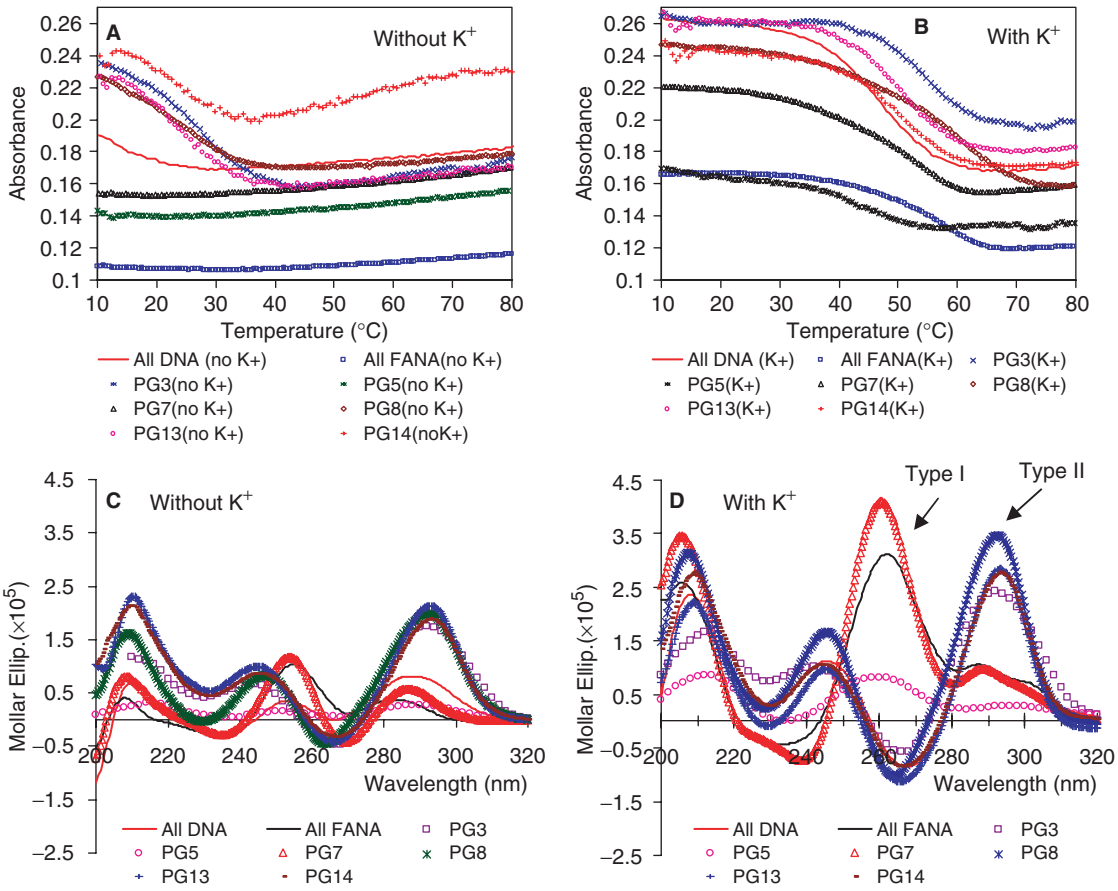

Figure 2. T_m profiles of selected 2′F-ANA-modified thrombin-binding aptamers (Table 1) measured at 295 nm in buffer 10 mM Tris, pH 6.8 (**A**) without KCl; (**B**) with 25 mM KCl, at a final strand concentration of 8 μM. The T_m data are provided in Table 1. CD spectra in the same buffer consisting of 10 mM Tris, pH 6.8 (**C**) without KCl; (**D**) with 25 mM KCl at 15°C at a final strand concentration of 8 μM. Type I and Type II CD types are shown in (**D**).

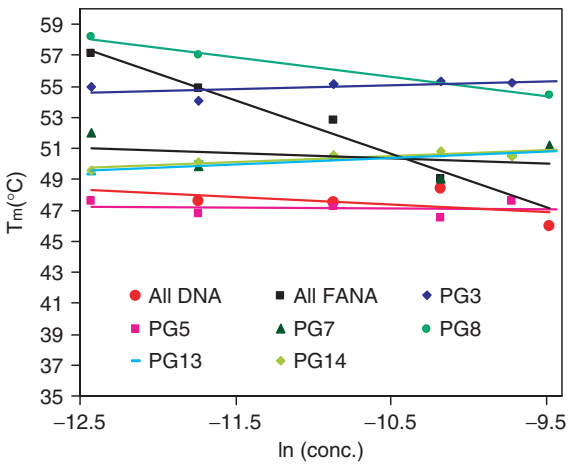

Figure 3. T_m versus concentration dependence (15–20-folds) study measured at 295 nm in a buffer consisting of 10 mM Tris, pH 6.8, 25 mM KCl for selected 2′F-ANA modified thrombin-binding aptamers (Table 1).

absorbance peak at 260 nm in the presence of K^+. Clearly this CD spectrum is Type I, which corresponds to a parallel quadruplex with all *anti*-Gs (11,12). A concentration-dependent T_m profile indicates the existence of intermolecular G-quadruplex formation (Figure 3). Even though we could not tell the existence of a dimeric or tetrameric G-quadruplex with all parallel strand alignments, it is clearly shown that all 2′F-ANA aptamer (PG2) could not maintain the unimolecular G-quadruplex topology (Figure 1B). An intermolecular G-quadruplex is thus formed to support a G-quartet structure with all *anti*-Gs. Hysteresis was observed in the heating and cooling processes, again supporting an intermolecular G-quadruplex adopted by PG2 (Figure 4).

Replacement of *anti*-Gs and *syn*-Gs with 2′F-ANA

Nucleotides with preferred glycosidic conformations have been utilized to investigate their effect on the topology and molecularity of G-tetrads. For example, 8-methyl-deoxyguanosine (8-Me-dG) and 8-bromodeoxyguanosine (8-Br-dG) which prefer *syn* conformation have demonstrated to play an important role in G-quadruplex conformation and thermal stability when they are used to modify a tetrameric G-quadruplex $[d(TGGGT)]_4$ (59,60). Recent studies by Tang and Shafer (61) demonstrate that ribonucleic acids which favor an *anti* conformation provide enough driving force to change the topology and molecularity for the thrombin-binding aptamer $d(G_2T_2G_2TGTG_2T_2G_2)$. A single locked nucleic

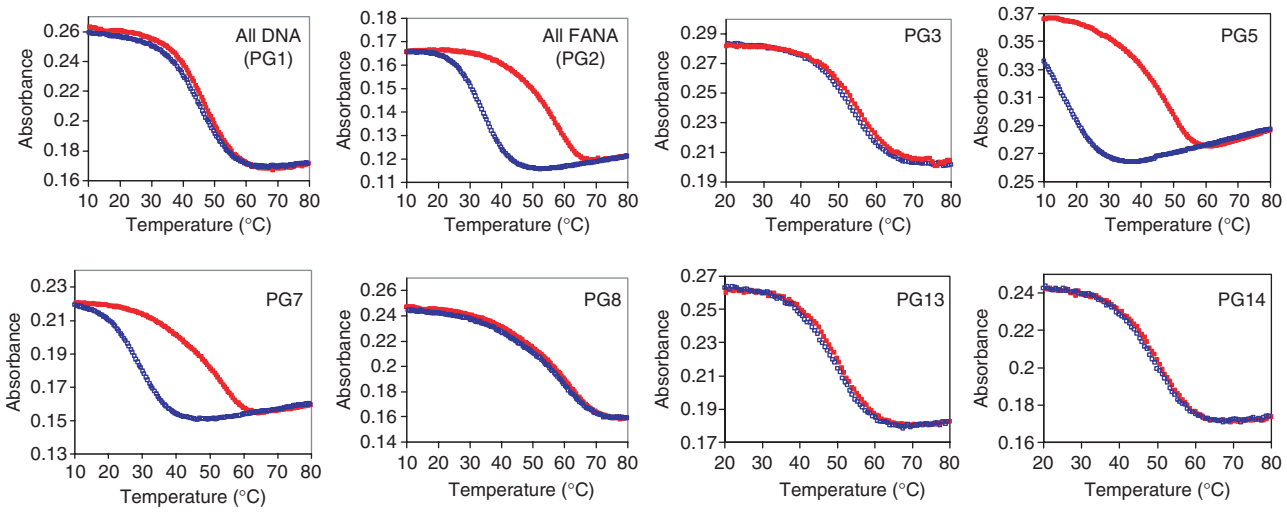

Figure 4. Heating and cooling T_m transitions of 2′F-ANA modified thrombin-binding aptamers (Table 1) measured at 295 nm in a buffer of 10 mM Tris, 25 mM KCl, pH 6.8, at a final strand concentration of 8 μM in a heating/cooling rate of 0.5°C/min (red filled square: heating; blue empty square: cooling).

acid (LNA) modification in an expected antiparallel folded quadruplex d($G_4(T_4G_4)_3$) has also been shown to induce a significant topological change to a parallel quadruplex in the presence of K^+ (62). 2′F-ANA unit which has been shown to have a conformationally biased sugar pucker (33) (i.e. more *south*/*east* than its DNA counterpart), is expected to favor an *anti* conformation in order to avoid steric interaction between guanine and the β-face fluorine (63) (Figure 5). Therefore, the next phase of the investigation was to study the effect of 2′F-araG on *anti*-Gs and *syn*-Gs observed in the different G-quadruplexes discussed earlier (see 'Introduction' section). We expected that the replacement of *anti*-Gs with 2′F-ANA would lead to thermal stabilization since preorganization of the *anti* glycosidic conformation favored by 2′F-araG (63) would reduce the loss of entropy during G-quartet assembly. Conversely, replacement of *syn*-Gs with 2′F-araGs is expected to cause destabilization or complete disruption of the G-quartet structure altogether.

The obtained T_m and CD data are consistent with the expected results. Modifying the *anti*-Gs with 2′F-ANA (PG3) or modifying both the *anti*-Gs and the loops with 2′F-ANA (PG4) increases thermal stability in the presence of K^+ ($\Delta T_m = +1.3$–1.5°C/2′F-ANA modification). The CD spectrum of PG3 was Type I CD, similar to the all DNA aptamer (PG1) (Figure 2C and D). Remarkably, PG4 shows a clear Type I CD both without and with K^+, demonstrating that the G-quadruplex adopted by PG4 could form even in the absence of K^+. In addition, it suggests that replacement of the loop with 2′F-ANA further benefits the G-quadruplex formation. This is consistent with previous work showing that all the thymidines in this thrombin-binding DNA aptamer adopt the *anti* orientation (15). A concentration-independent T_m profile (Figure 3) and lack of hysteresis in heating/cooling processes both support a unimolecular G-quadruplex structure like the DNA control (Figure 4 and Figure S1 in Supplementary Data). Replacement of *anti*-G with 2′F-ANA is therefore able to stabilize the G-quartet without changing the quadruplex topology.

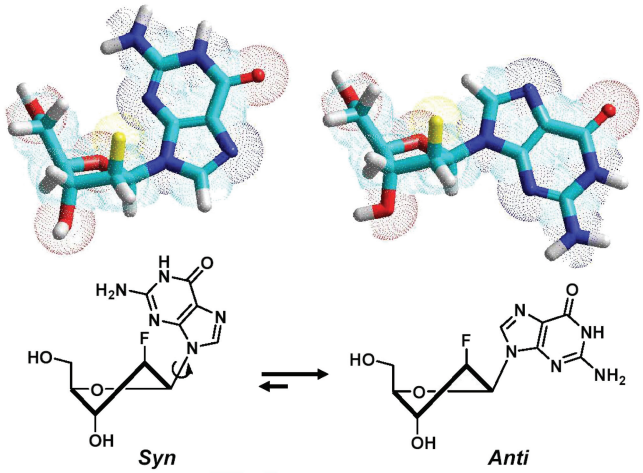

Figure 5. Glycosic conformation equilibrium of dG and 2′F-araG with south furanose sugar ring.

The results of replacement of the *syn*-Gs with 2′F-ANA also match expectations. Modification of the *syn*-Gs with 2′F-ANA (PG5) and replacement of both *syn*-Gs and loops (PG6) with 2′F-ANA result in less stable complexes compared with PG3 and PG4. PG5 is even less stable than the original all DNA aptamer ($\Delta T_m = -0.5$°C/2′F-ANA modification, Table 1), and PG6 is only as stable as the all DNA aptamer control ($\Delta T_m = +0.1$°C/2′F-ANA modification, Table 1). CD experiments show that both PG5 and PG6 display very low amplitude peaks at 260 nm even in the presence of K^+, indicating little structure formed (Figure 2C and D and Figure S4 in Supplementary Data). A T_m versus concentration study suggested that the T_m of PG5 and PG6 is independent of concentration so they likely still form unimolecular structures (Figure 3) but the

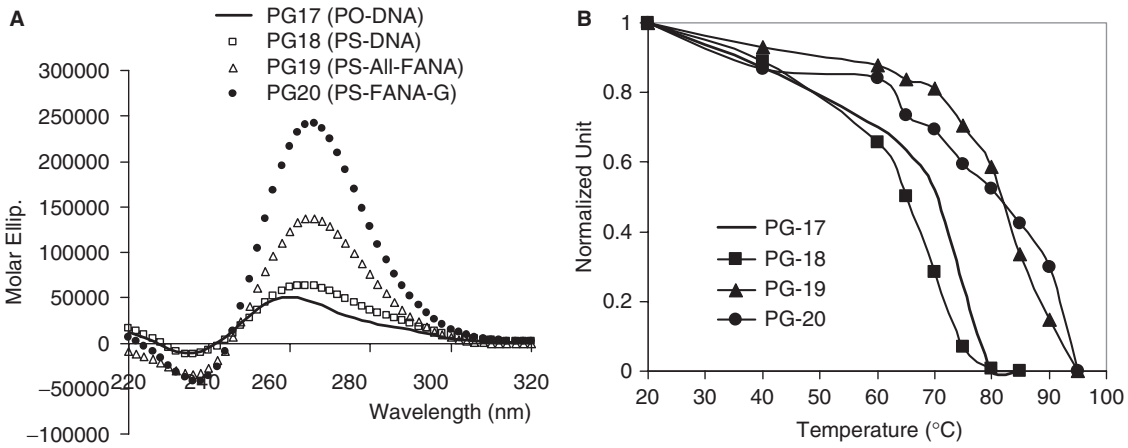

Figure 6. (**A**) CD spectra of $dT_2G_4T_2$ and related sequences (PG17–20) obtained in PBS buffer at a strand concentration of 20 μM (single strand). (**B**) T_m curves generated by plotting the maximum absorbance at 265 nm wavelength (normalized) versus temperature in a series of CD-temperature-dependent measurements (Figure S5, Supplementary Data); the corresponding T_m data are shown in Table 2.

formation of these structures seems kinetically slow based on the finding that major hysteresis is observed at a heating/cooling rate of 0.5°C/min (Figure 4 and Figure S1 in Supplementary Data). Taken together, if the unimolecular G-quadruplex is maintained in PG5 and PG6, the folding topology should be changed to tolerate a unimolecular all-parallel G-quadruplex structure with all *anti*-Gs indicated by a Type I CD profile. A parallel unimolecular quadruplex has been demonstrated in an X-ray crystal structure of the human telomere sequence $d(AG_3(TTAG_3)_3)$ by Neidle and coworkers (64) and in a LNA modified $d(G_4(T_4G_4)_3)$ quadruplex by Dominick and Jarstfer (62). It seems that this atypical folding in PG5 and PG6 is not favored since the defined structure is not present in significant quantity in solution, as indicated by the previous CD experiments. The possible reason could be the loop size and sequences which are important factors in determining the folding topology (64). Furthermore, in the case where 2′F-araGs replace both *syn*-Gs and *anti*-Gs in the quartet (PG7), we found that 2′F-ANA brings minimal stabilization ($\Delta T_m = +0.4$°C/2′F-ANA modification, Table 1). Type I CD profile (i.e. a positive CD band at ~260 nm and a negative band at ~240 nm) was observed in the presence of K^+ and not shown in the absence of K^+, indicating a parallel quadruplex with all *anti*-Gs (12), as in PG2. Concentration-dependent T_m (Figure 3) and significant hysteresis observed in heating/cooling processes (Figure 4) support the idea that PG7 could adopt an intermolecular parallel G-quadruplex with all *anti*-Gs. Further non-denaturing shift gel analysis experiments are needed to confirm the molecularity of intermolecular G-quadruplexes studied here.

To verify whether *anti*-Gs can be stabilized by 2′F-ANA in other types of G-quadruplexes, we chose two other aptamers from the literature.

(A) *Anti-HIV phosphorothioate PS-d($T_2G_4T_2$) modified with 2′F-ANA*. Both the phosphodiester sequence PO-$d(T_2G_4T_2)$ and the phosphorothioate sequence PS-$d(T_2G_4T_2)$ are known to adopt a structure in which all G residues are in the *anti* conformation (7,43). As a result, this aptamer has a characteristic 'Type I' CD signature (Table 2 and Figure 6A) (12). Thermal denaturation studies at 260 nm yielded noisy curves. The reason for this could be the slow dissociation process of both phosphodiester and phosphorothioate as reported in the literature (43). T_m profiles shown in Figure 6B were obtained by plotting the maximum molar ellipticities versus temperature based on temperature-dependent CD spectra (Figure S5, Supplementary Data). Although it is impossible to get accurate T_m data for these kinetically slow G-quadruplexes, clearly our apparent T_m data help to confirm the significant thermal stabilization provided by the 2′F-ANA-G units (PG18–20, Table 2). Our results indicate that phosphorothioate modifications lead to stabilization, inconsistent with the literature finding (31). Compared with the controls PG17 (PO-DNA) and PG18 (PS-DNA), 2′F-ANA modified sequences PG19 and PG20 show large increases in molar ellipticities, indicating a better guanine–guanine interactions within the G-quartet structure.

(B) *A telomeric DNA d($G_4T_4G_4$) modified with 2′F-ANA*. Structural analysis has shown that a telomeric DNA sequence $d(G_4T_4G_4)$ (PG21, Table 2) can form a symmetrical dimeric quadruplex with four G-quartets and a diagonal loop in the presence of Na^+ (Figure 1C) (21,22). The guanine conformation is 5′-$d(G_sG_aG_sG_a$-TTTT-$G_sG_aG_sG_a)$-3′ where *s* denotes *syn* and *a anti* (22,25). Several sequences, including a fully 2′F-ANA modified sequence (PG22), a sequence with 2′F-ANA replacing all *syn*-Gs (PG23) and a sequence with 2′F-ANA modifications for all *anti*-Gs (PG24), were tested (Table 2). When the *anti*-G residues were replaced by 2′F-ANA G residues, a modest thermal stabilization of the G-quadruplex structure resulted, without disruption of the 3D structure (Table 2, and Figure 7A and B). When the *syn*-G residues were replaced (PG22 and PG23), a remarkable increase in thermal stabilization of the G-quadruplex structure resulted (up to 25°C; Table 2), with a concomitant Type II-to-Type I conformational change induced by the 2′F-ANA-G(*anti*) replacement (Figure 7A).

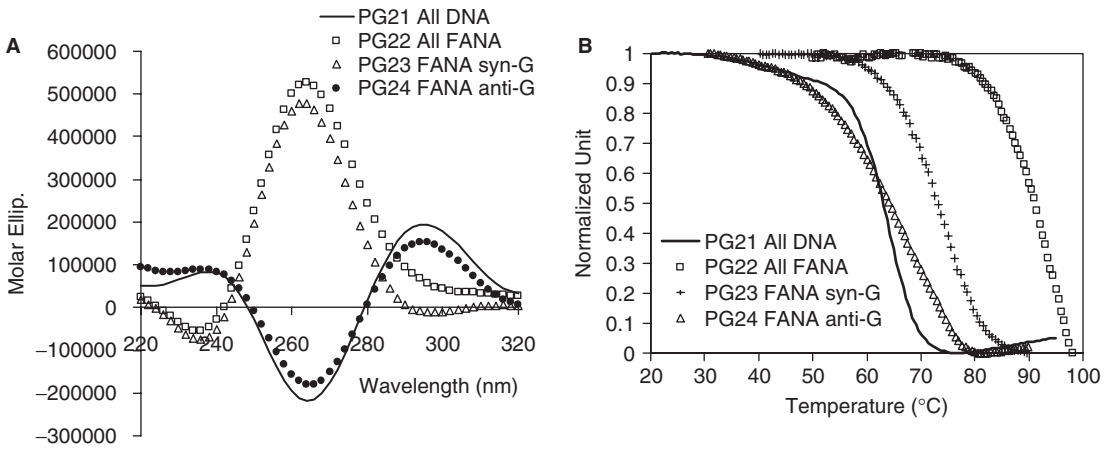

Figure 7. (**A**) CD spectra of $dT_4G_4T_4$ and related sequences (PG21–24) in 10 mM sodium phosphate buffer, 0.1 mM EDTA, pH 7 and 200 mM NaCl at a strand concentration of 10 μM. (**B**) T_m profile measured at 295 nm in the same sodium phosphate buffer at a strand concentration of 100 μM.

Overall, these two additional examples confirm the results obtained for the thrombin-binding aptamers: the modification of *anti*-Gs with 2′F-ANA can generally stabilize a G-quartet requiring *anti*-Gs, maintaining the overall quadruplex conformation, while the modification of *syn*-Gs with 2′F-ANA is not favored and results in a complete conformational switch to an alternative G-quadruplex structure, as indicated by the change of CD type from II to I for PG2, PG5, PG6, PG7, PG22 and PG23 (Tables 1 and 2, Figure 2D, Figure 7A and Figure S4 in Supplementary Data). The stabilizing effects of 2′F-ANA on G-quadruplexes is related to the conformational preorganization and the small steric effect of the fluorine atom. 2′-*O*-Methyl modification generates steric problems at the 2′ position and is often shown to destabilize a unimolecular G-quadruplex, resulting in significant conformational perturbation in both intra- and intermolecular G-quadruplex systems (31). The ability to switch G-quartet structures with a β-fluorine atom may be exploited to enrich the population of one of several interconverting G-quadruplex conformations (a β-fluorine ''switch'').

Replacement of loops with 2′F-ANA

Thymine bases in the loop region of the thrombin-binding aptamer $d(G_1G_2T_3T_4G_5G_6T_7G_8T_9G_{10}G_{11}T_{12}T_{13}G_{14}G_{15})$ (Figure 1B) exclusively prefers the *anti* orientation (15). The literature reports that G_8 shows base stacking interactions with the first G-quartet but the conformation of the nucleotide was not mentioned (18). The replacement of G_8 with 2′F-araG in this study resulted in an increase of 0.8°C in T_m (PG8 and PG9 in Table 1). It was expected that the replacement of *anti* thymines in the loops with *anti* conformationally biased 2′F-araT should increase thermal stability. Thermal melting studies support this hypothesis (PG8–14, Table 1). Different positions of thymidine contribute to the stability of the G-quadruplex to different degrees (Table 1 and Figure S2, Supplementary Data). 2′F-ANA replacements in the loops consisting of two thymidines (PG12) bring a greater thermal stabilization (ΔT_m = 2.9°C/2′F-ANA modification, Table 1) than with modification in the TGT loop (PG9, ΔT_m = 1.6°C/2′F-ANA modification, Table 1). T_3 and T_{12} are the most sensitive positions to 2′F-araT modification resulting in an almost 6°C difference in T_m (PG9 versus PG10; PG11 versus PG14, Table 2), while the replacement of T_{13} and T_4 with 2′F-araT is much less sensitive and results only in slight T_m increases of 1°C (PG9 versus PG11, Table 2) and 0.2°C (PG10 versus PG13, Table 2), respectively. The crystal structure of this DNA aptamer bound to thrombin suggests that T_3 and T_{12} are different from T_4 and T_{13}. It appears that the bases of T_3 and T_{12} do not interact with any other moieties within the aptamer, nor do they interact with thrombin, instead, they extend out into the solvent (18). Modifying T_3 and T_{12} with 2′F-araT might change the conformation of the loops, bringing out stabilization to the whole G-quadruplex structure as suggested by the T_m increase. A detailed picture, however, is difficult to describe at this stage. The replacement of the central nucleotide G_8 with a 2′F-araG is also less important for stabilization (PG8 versus PG9, only 0.8°C T_m difference). Overall, 2′F-ANA modifications of loop deoxynucleotides stabilizes the formation of a unimolecular G-quadruplex (Figure 1B), as supported by all CD and UV melting analysis. It was found that all loop-modified thrombin-binding aptamers (PG8–14) maintain Type II CD in the presence of K^+, like the DNA aptamer control (Figure S4, Supplementary Data). Remarkably, in the absence of K^+, a relatively strong positive peak at ~295 nm is still observed, which indicates significant G-quartet formation. Therefore, replacement of the loop deoxynucleotides with 2′F-ANA significantly helps with the formation of G-quadruplex structure. They show concentration-independent T_m data, indicating a unimolecular structure, in agreement with a lack of hysteresis in heating/cooling processes (Figure 4 and Figure S1, Supplementary Data).

Nuclease resistance induced by 2′F-ANA

Incorporation of 2′F-ANA in oligonucleotides leads to an improvement in nuclease resistance (34). This study

further evaluates the nuclease resistance of fully 2′F-ANA-modified thrombin-binding aptamers (PG1–14, Table 1). The data clearly shows that 2′F-ANA modified aptamers have enhanced half-lives in 10% FBS (in some cases >48-fold compared with PG1, Figure S6 in Supplementary Data and Table 1) but nuclease stability is found to be dependent on both the position (esp. *syn*-G and *anti*-G) and number of 2′F-ANA residues within the oligonucleotide backbone. For example, replacing *anti*-Gs with 2′F-ANA (PG3 and PG4) increases the half-lives to 4.8 and 9.4 h, respectively, while replacing *syn*-Gs with 2′F-ANA (PG5 and PG6) does not yield much gain in biostability with half-life increases of only 0.8 and 0.6 h, respectively, comparable to the DNA aptamer (PG1) (Figure S6 in Supplementary Data and Table 1). These differences could be justified by the previous finding that PG5 and PG6 only form insignificant G-quadruplex structures (Figure 2D) due to the unfavored conformation of the perturbed *syn*-Gs. It is expected that a complex structure should be less accessible for nuclease attack compared to dissociated or 'open' oligonucleotides. Furthermore, the nuclease stability of PG13 and PG14 is enhanced over PG1 by a factor of 4–7 with only four 2′F-ANA incorporated (Table 1). Modification of the loop residues of stable structures (e.g. PG4, PG8) may have a double effect since the increased stability of the duplex would be combined with protection of the nucleotides most exposed to endonuclease attack.

Binding affinity of 2′F-ANA-modified thrombin-binding aptamers with thrombin

As mentioned in the 'Introduction' section, the structure of the thrombin-binding aptamer is very sensitive to chemical modifications, which often undermine its thermal stability and/or binding activity (31). Thus, a final experiment in this study was conducted using nitrocellulose filter binding assays to assess the effect of 2′F-ANA modifications on the thrombin binding affinity. Data are presented in Table 1 and in Figure 8. ssDNA (P8) and hairpin (H1) controls show no binding to thrombin as expected (18). Binding of 2′F-ANA aptamers to thrombin is always adversely affected by 2′F-ANA modifications on G-quartets themselves, whether *syn*- or *anti*-Gs are modified (PG2-PG6). Some loop modifications with 2′F-ANA also disfavor thrombin binding (PG8–PG12). However, two loop-modified aptamers (PG13 and PG14, Table 1) show a 4–5-fold enhancement in thrombin-binding affinity. This conclusion should bear in mind that while these two aptamers may have enhanced binding affinity, the slope of the concentration response is not as sharp as that for the native PG1. Therefore, this study reveals the first 2′F-ANA modified thrombin-binding aptamers to combine enhanced thermal and nuclease stability with apparently slightly stronger binding affinity. Previous structural studies by NMR and crystallography suggest that the loop moieties would change conformation during binding to thrombin (18). The TGT loop is involved with the fibrinogen exosite and two TT loops could interact with the heparin exosite. It seems therefore that two 2′F-ANA-T residues when present in one of the TT loops and the TGT loop enhance thrombin binding.

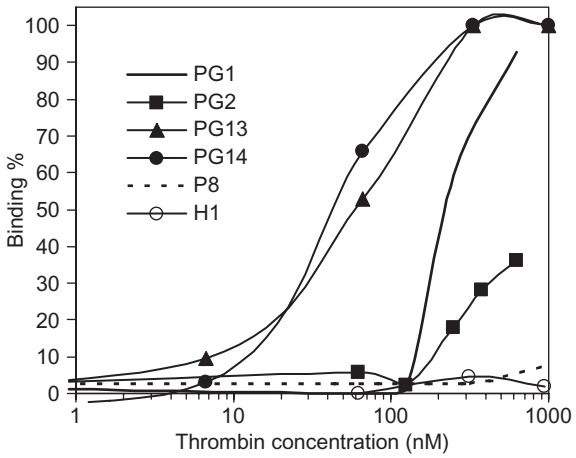

Figure 8. Binding affinity of selected aptamers with human thrombin assessed by nitrocellulose filter binding assays.

CONCLUSIONS

In the present study 2′F-ANA modified oligonucleotides were investigated based on a thrombin-binding DNA aptamer d($G_2T_2G_2TGTG_2T_2G_2$), an anti-HIV phosphothioate PS-d($T_2G_4T_2$) and a DNA telomeric sequence d($G_4T_4G_4$) (Tables 1 and 2) by UV thermal denaturation and CD experiments. Generally, replacement of *anti*-Gs with 2′F-ANA can stabilize a G-quartet requiring *anti*-Gs and maintain the quadruplex conformation, while replacement of *syn*-Gs with 2′F-ANA is not favored and results in complete conformational change of the G-quadruplexes. The data shows that appropriate incorporation of 2′F-ANA residues into G-quadruplexes leads to an increase in the melting temperature of the complex formed (ΔT_m up to $\sim+3^{\circ}$C/2′F-ANA modification, Tables 1 and 2). The structure of thrombin-binding aptamers is stabilized by the presence of potassium ions. Nuclease resistance of 2′F-ANA modified thrombin-binding aptamers is increased up to 48-fold in 10% FBS. Two 2′F-ANA-modified thrombin-binding aptamers (PG13 and PG14) show a 4–5-fold enhancement in binding affinity to thrombin along with increased thermal stability and nuclease resistance. Therefore, the impact of 2′F-ANA modifications on G-quartets and loop regions has been demonstrated. The study suggests that 2′F-ANA may positively impact oligonucleotide-based therapeutics involving G-quadruplexes.

SUPPLEMENTARY DATA

Supplementary Data are available at NAR Online.

ACKNOWLEDGEMENTS

We acknowledge financial support through a grant from the Canadian Institutes of Health Research (CIHR) and Topigen Pharmaceuticals, Inc. CGP acknowledges

support from a FQRNT fellowship and a Clifford Wong McGill Major Fellowship. We thank J. Watts, R. Donga and J. Lackey for helpful feedback during the preparation of this manuscript. C. G. P. and M.J.D. are recipients of the Carl Winkler Dissertation Award (McGill University) and Bernard Belleau Award (Canadian Society for Chemistry), respectively. Funding to pay the Open Access publication charges for this article was provided by CIHR (Canadian Institutes of Health Research). Dedicated to Hermano Juan Antón on the occasion of his 61th birthday.

Conflict of interest statement. None declared.

REFERENCES

1. Gellert,M., Lipsett,M.N. and Davies,D.R. (1962) Helix formation by guanylic acid. *Proc. Natl Acad. Sci. USA*, **48**, 2013–2018.
2. Sen,D. and Gilbert,W. (1988) Formation of parallel 4-stranded complexes by guanine-rich motifs in DNA and its implications for meiosis. *Nature*, **334**, 364–366.
3. Tuerk,C. and Gold,L. (1990) Systematic evolution of ligands by exponential enrichment: RNA ligands to bacteriophage T4 DNA polymerase. *Science*, **249**, 505–510.
4. Ellington,A.D. and Szostak,J.W. (1990) I*n vitro* selection of RNA molecules that bind specific ligands. *Nature*, **346**, 818–822.
5. Joyce,G.F. (1989) Amplification, mutation and selection of catalytic RNA. *Gene*, **82**, 83–87.
6. Bock,L.C., Griffin,L.C., Latham,J.A., Vermaas,E.H. and Toole,J.J. (1992) Selection of single-stranded DNA molecules that bind and inhibit human thrombin. *Nature*, **355**, 564–566.
7. Wyatt,J.R., Vickers,T.A., Roberson,J.L., Buckheit,R.W., Klimkait,T., Debaets,E., Davis,P.W., Rayner,B., Imbach,J.L. *et al.* (1994) Combinatorially selected guanosine-quartet structure is a potent inhibitor of human-immunodeficiency-virus envelope-mediated cell-fusion. *Proc. Natl Acad. Sci. USA*, **91**, 1356–1360.
8. Phan,A.T., Kuryavyi,V., Ma,J.B., Faure,A., Andreola,M.L. and Patel,D.J. (2005) An interlocked dimeric parallel-stranded DNA quadruplex: a potent inhibitor of HIV-1 integrase. *Proc. Natl Acad. Sci. USA*, **102**, 634–639.
9. Jing,N.J. and Hogan,M.E. (1998) Structure-activity of tetrad-forming oligonucleotides as a potent anti-HIV therapeutic drug. *J. Biol. Chem.*, **273**, 34992–34999.
10. Borman,S. (2006) Targeting telomerase. *Chem. Eng. News*, **84**, 32–33.
11. Keniry,M.A. (2000) Quadruplex structures in nucleic acids. *Biopolymers*, **56**, 123–146.
12. Williamson,J.R. (1994) G-quartet structures in telomeric DNA. *Annu. Rev. Biophys. Biomol. Struct.*, **23**, 703–730.
13. Kerwin,S.M. (2000) G-quadruplex DNA as a target for drug design. *Curr. Pharm. Des.*, **6**, 441–471.
14. Schultze,P., Macaya,R.F. and Feigon,J. (1994) Three-dimensional solution structure of the thrombin-binding DNA aptamer d(GGTTGGTGTGGTTGG). *J. Mol. Biol.*, **235**, 1532–1547.
15. Macaya,R.F., Schultze,P., Smith,F.W., Roe,J.A. and Feigon,J. (1993) Thrombin-binding DNA aptamer forms a unimolecular quadruplex structure in solution. *Proc. Natl Acad. Sci. USA*, **90**, 3745–3749.
16. Wang,K.Y., Mccurdy,S., Shea,R.G., Swaminathan,S. and Bolton,P.H. (1993) A DNA aptamer which binds to and inhibits thrombin exhibits a new structural motif for DNA. *Biochemistry*, **32**, 1899–1904.
17. Wang,K.Y., Krawczyk,S.H., Bischofberger,N., Swaminathan,S. and Bolton,P.H. (1993) The tertiary structure of a DNA aptamer which binds to and inhibits thrombin determines activity. *Biochemistry*, **32**, 11285–11292.
18. Padmanabhan,K., Padmanabhan,K.P., Ferrara,J.D., Sadler,J.E. and Tulinsky,A. (1993) The structure of alpha-thrombin inhibited by a 15-mer single-stranded DNA aptamer. *J. Biol. Chem.*, **268**, 17651–17654.
19. Padmanabhan,K. and Tulinsky,A. (1996) An ambiguous structure of a DNA 15-mer thrombin complex. *Acta Crystallogr. D Biol. Crystallogr.*, **D52**, 272–282.
20. Kelly,J.A., Feigon,J. and Yeates,T.O. (1996) Reconciliation of the x-ray and NMR structures of the thrombin-binding aptamer d(GGTTGGTGTGGTTGG). *J. Mol. Biol.*, **256**, 417–422.
21. Schultze,P., Smith,F.W. and Feigon,J. (1994) Refined solution structure of the dimeric quadruplex formed from the *Oxytricha* telomeric oligonucleotide d(GGGGTTTTGGGG). *Structure*, **2**, 221–233.
22. Smith,F.W. and Feigon,J. (1992) Quadruplex structure of *Oxytricha* telomeric DNA oligonucleotides. *Nature*, **356**, 164–168.
23. Kang,C., Zhang,X.H., Ratliff,R., Moyzis,R. and Rich,A. (1992) Crystal structure of 4 stranded *Oxytricha* telomeric DNA. *Nature*, **356**, 126–131.
24. Haider,S., Parkinson,G.N. and Neidle,S. (2002) Crystal structure of the potassium form of an Oxytricha nova G-quadruplex. *J. Mol. Biol.*, **320**, 189–200.
25. Schultze,P., Hud,N.V., Smith,F.W. and Feigon,J. (1999) The effect of sodium, potassium and ammonium ions on the conformation of the dimeric quadruplex formed by the *Oxytricha nova* telomere repeat oligonucleotide d($G_4T_4G_4$). *Nucleic Acids Res.*, **27**, 3018–3028.
26. Hardin,C.C., Perry,A.G. and White,K. (2000) Thermodynamic and kinetic characterization of the dissociation and assembly of quadruplex nucleic acids. *Biopolymers*, **56**, 147–194.
27. Heckel,A. and Mayer,G. (2005) Light regulation of aptamer activity: an anti-thrombin aptamer with caged thymidine nucleobases. *J. Am. Chem. Soc.*, **127**, 822–823.
28. Di Giusto,D.A. and King,G.C. (2004) Construction, stability, and activity of multivalent circular anticoagulant aptamers. *J. Biol. Chem.*, **279**, 46483–46489.
29. Buijsman,R.C., Schipperijn,J.W.J., Kuyl-Yeheskiely,E., Van Der Marel,G.A., Van Boeckel,C.A.A. and Van Boom,J.H. (1997) Design and synthesis of a possible mimic of a thrombin-binding DNA aptamer. *Bioorg. Med. Chem. Lett.*, **7**, 2027–2032.
30. Rosemeyer,H., Mokrosch,V., Jawalekar,A., Becker,E.-M. and Seela,F. (2004) Single-stranded DNA: replacement of canonical by base-modified nucleosides in the minihairpin 5′-d(GCGAAGC)-3′ and constructs with the aptamer 5′-d(GGTTGGTGTGGTTGG)-3′. *Helv. Chim. Acta*, **87**, 536–553.
31. Sacca,B., Lacroix,L. and Mergny,J.-L. (2005) The effect of chemical modifications on the thermal stability of different G-quadruplex-forming oligonucleotides. *Nucleic Acids Res.*, **33**, 1182–1192.
32. Lebruska,L.L. and Maher,L.J.III. (1999) Selection and characterization of an RNA decoy for rranscription factor NF-kB. *Biochemistry*, **38**, 3168–3174.
33. Trempe,J.-F., Wilds,C.J., Denisov,A.Y., Pon,R.T., Damha,M.J. and Gehring,K. (2001) NMR solution structure of an oligonucleotide hairpin with a 2′F-ANA/RNA stem: implications for RNase H specificity toward DNA/RNA hybrid duplexes. *J. Am. Chem. Soc.*, **123**, 4896–4903.
34. Kalota,A., Karabon,L., Swider,C.R., Viazovkina,E., Elzagheid,M., Damha,M.J. and Gewirtz,A.M. (2006) 2′-Deoxy-2′-fluoro-beta-D-arabinonucleic acid (2′F-ANA) modified oligonucleotides (ON) effect highly efficient, and persistent, gene silencing. *Nucleic Acids Res.*, **34**, 451–461.
35. Wilds,C.J. and Damha,M.J. (2000) 2′-Deoxy-2′-fluoro-β-D-arabinonucleosides and olignucleotides (2′F-ANA): synthesis and physicochemical studies. *Nucleic Acids Res.*, **28**, 3625–3635.
36. Wilds,C.J. and Damha,M.J. (1999) Duplex recognition by oligonucleotides containing 2′-deoxy-2′-fluoro-D-arabinose and 2′-deoxy-2′-fluoro-D-ribose. Intermolecular 2′-OH-phosphate contacts versus sugar puckering in the stabilization of triple-helical complexes. *Bioconjug. Chem.*, **10**, 299–305.
37. Wilds,C.J. (2000) *Ph.D. Thesis.* McGill University, Montreal.
38. Lok,C.-N., Viazovkina,E., Min,K.-L., Nagy,E., Wilds,C.J., Damha,M.J. and Parniak,M.A. (2002) Potent gene-specific inhibitory properties of mixed-backbone antisense oligonucleotides comprised of 2′-deoxy-2′-fluoro-D-arabinose and 2′-deoxyribose nucleotides. *Biochemistry*, **41**, 3457–3467.
39. Dowler,T., Bergeron,D., Tedeschi,A.L., Paquet,L., Ferrari,N. and Damha,M.J. (2006) Improvements in siRNA properties mediated by

2′-deoxy-2′-fluoro-beta-D-arabinonucleic acid (FANA). *Nucleic Acids Res.*, **34**, 1669–1675.
40. Watts,J.K., Choubdar,N., Sadalapure,K., Robert,F., Wahba,A.S., Pelletier,J., Pinto,B.M. and Damha,M.J. (2007) 2′-Fluoro-4′-thioarabino-modified oligonucleotides: conformational switches linked to siRNA activity. *Nucleic Acids Res.*, **35**, 1441–1451.
41. Viazovkina,E.V., Mangos,M.M., Elzagheid,M.I. and Damha,M.J. (2002) *Current Protocols in Nucleic Acid Chemistry*, John Wiley & Sons, Inc. pp. 4.15.11–22.
42. Smirnov,I. and Shafer,R.H. (2000) Effect of loop sequence and size on DNA aptamer stability. *Biochemistry*, **39**, 1462–1468.
43. Wyatt,J.R., Davis,P.W. and Freier,S.M. (1996) Kinetics of G-quartet-mediated tetramer formation. *Biochemistry*, **35**, 8002–8008.
44. Lu,M., Guo,Q. and Kallenbach,N.R. (1993) Thermodynamics of G-tetraplex formation by telomeric DNAs. *Biochemistry*, **32**, 598–601.
45. Cantor,C.R., Warshaw,M.M. and Shapiro,H. (1970) Oligonucleotide interactions. 3. Circular dichroism studies of conformation of deoxyoligonucleotides. *Biopolymers*, **9**, 1059–1077.
46. Galarneau,A., Min,K.-L., Mangos,M.M. and Damha,M.J. (2005) *Methods Mol. Biol.* Totowa, NJ, United States, Vol. 288, pp. 65–80.
47. Nimjee,S.M., Rusconi,C.P. and Sullenger,B.A. (2005) Aptamers: an emerging class of therapeutics. *Annu. Rev. Med.*, **56**, 555–583.
48. Brody,E.N. and Gold,L. (2000) Aptamers as therapeutic and diagnostic agents. *Rev. Mol. Biotechnol.*, **74**, 5–13.
49. White,R.R., Sullenger,B.A. and Rusconi,C.P. (2000) Developing aptamers into therapeutics. *J. Clin. Invest.*, **106**, 929–934.
50. Pestourie,C., Tavitian,B. and Duconge,F. (2005) Aptamers against extracellular targets for in vivo applications. *Biochimie*, **87**, 921–930.
51. Nolte,A., Klussmann,S., Bald,R., Erdmann,V.A. and Fuerste,J.P. (1996) Mirror-design of L-oligonucleotide ligands binding to L-arginine. *Nat. Biotechnol.*, **14**, 1116–1119.
52. Ruckman,J., Green,L.S., Beeson,J., Waugh,S., Gillette,W.L., Henninger,D.D., Claesson-Welsh,L. and Janjic,N. (1998) 2′-Fluoropyrimidine RNA-based aptamers to the 165-amino acid form of vascular endothelial growth factor (VEGF165). Inhibition of receptor binding and VEGF-induced vascular permeability through interactions requiring the exon 7-encoded domain. *J. Biol. Chem.*, **273**, 20556–20567.
53. Lato,S.M., Ozerova,N.D.S., He,K., Sergueeva,Z., Shaw,B.R. and Burke,D.H. (2002) Boron-containing aptamers to ATP. *Nucleic Acids Res.*, **30**, 1401–1407.
54. Kato,Y., Minakawa,N., Komatsu,Y., Kamiya,H., Ogawa,N., Harashima,H. and Matsuda,A. (2005) New NTP analogs: the synthesis of 4′-thioUTP and 4′-thioCTP and their utility for SELEX. *Nucleic Acids Res.*, **33**, 2942–2951.
55. Jhaveri,S., Olwin,B. and Ellington,A.D. (1998) *In vitro* selection of phosphorothiolated aptamers. *Bioorg. Med. Chem. Lett.*, **8**, 2285–2290.
56. Pagratis,N.C., Bell,C., Chang,Y.-F., Jennings,S., Fitzwater,T., Jellinek,D. and Dang,C. (1997) Potent 2′-amino-, and 2′-fluoro-2′-deoxyribonucleotide RNA inhibitors of keratinocyte growth factor. *Nat. Biotechnol.*, **15**, 68–73.
57. Ng,E.W.M., Shima,D.T., Calias,P., Cunningham,E.T., Guyer,D.R. and Adamis,A.P. (2006) Pegaptanib, a targeted anti-VEGF aptamer for ocular vascular disease. *Nat. Rev. Drug Discov.*, **5**, 123–132.
58. Mergny,J.L., Phan,A.T. and Lacroix,L. (1998) Following G-quartet formation by UV-spectroscopy. *FEBS Lett.*, **435**, 74–78.
59. Virgilio,A., Esposito,V., Randazzo,A., Mayol,L. and Galeone,A. (2005) 8-Methyl-2′-deoxyguanosine incorporation into parallel DNA quadruplex structures. *Nucleic Acids Res.*, **33**, 6188–6195.
60. Esposito,V., Randazzo,A., Piccialli,G., Petraccone,L., Giancola,C. and Mayol,L. (2004) Effects of an 8-bromodeoxyguanosine incorporation on the parallel quadruplex structure [d(TGGGT)](4). *Org. Biomol. Chem.*, **2**, 313–318.
61. Tang,C.F. and Shafer,R.H. (2006) Engineering the quadruplex fold: Nucleoside conformation determines both folding topology and molecularity in guanine quadruplexes. *J. Am. Chem. Soc.*, **128**, 5966–5973.
62. Dominick,P.K. and Jarstfer,M.B. (2004) A conformationally constrained nucleotide analogue controls the folding topology of a DNA G-quadruplex. *J. Am. Chem. Soc.*, **126**, 5050–5051.
63. Sapse,A.M. and Snyder,G. (1985) Ab initio studies of the antiviral drug 1-(2-fluoro-2-deoxy-beta-D-arabinofuranosyl) thymine. *Cancer Invest.*, **3**, 115–121.
64. Parkinson,G.N., Lee,M.P.H. and Neidle,S. (2002) Crystal structure of parallel quadruplexes from human telomeric DNA. *Nature*, **417**, 876–880.